Article

Combretastatin A-4: The Antitubulin Agent that Inspired the Design and Synthesis of Styrene and Spiroisatin Hybrids as Promising Cytotoxic, Antifungal and Antiviral Compounds

Yaneth M. Brand, [iD] **,a Vladimir V. Kouznetsov,* [iD] *b Carlos E. Puerto,* [iD] *b,c*
Vicky C. R. Linares, [iD] *a Verónica T. Castaño*a *and Liliana Betancur-Galvis*a

aGroup of Investigative Dermatology, Institute of Medicinal Research, Medicine Faculty, University of Antioquia, 1226, 050022 Medellín, Colombia

bLaboratorio de Química Orgánica y Biomolecular, Centro de Materiales y Nanociencias (CMN), Parque Tecnológico Guatiguará, Universidad Industrial de Santander, km 2 vía Refugio, A.A. 681011 Piedecuesta, Colombia

cLaboratorio de Química Orgánica Aplicada, Universidad Manuela Beltrán, Cl. 33 No. 26-34, A.A. 680002 Bucaramanga, Colombia

The design of a series of styrene and spiroisatin hybrids was based on the structure of combretastatin A-4 **1**. This library of 20 compounds were synthesized with the pharmacophoric units: 3,4,5-trimethoxy or/and 4-hydroxy-3-methoxy phenyl moities in their structure. Thereby, the libraries of β-nitrostyrenes **10a**-**10c**, spiroisatin-dihydroquinolines **14a**-**14c**, spiroisatin-thiazolidinones **17a**-**17c** and spiroisatin-nitropyrrolidizines **20a**-**20k** were evaluated for their *in vitro* cytotoxic, anti-proliferative, antifungal and antiviral activities. Biological results revealed that among these compounds, β-nitrostyrenes **10a**-**10c** exhibited significant cytotoxicity (HeLa and Jurkat tumor cells) and antifungal (*T. mentagrophytes*) activities. Moreover, the spiroisatin-dihydroquinoline **14a** and **14c** showed promising cytotoxicity (U937 cells). **14a**-**14c** molecules were active against human herpesviruses serotypes 1 and 2 (HHV-1 and HHV-2), but only **14a** and **14b** were effective against dengue virus serotype 2 (DENV-2). The spiroisatin-nitropyrrolidizine **20c** exhibited moderate anti-herpetic activity, while **17c** spiroisatin-thiazolidinone derivative also reduced the infection of HHV-1 and DENV-2. Finally, the molecular docking showed that these kind of molecules interact with the subunit α/β-tubulin.

Keywords: combretastatin A-4, β-nitrostyrenes, spiroisatin hybrids, anti-proliferative, antifungal and antiviral activities

Introduction

Combretastatin A-4 **1** (CA-4), the most potent and studied compound isolated from the bark of the South African willow tree *Combretum caffrum*,[1] stands out among other members of the combretastatin family due to its cytotoxic properties as inhibitor of angiogenesis and tubulin polymerization.[2]

The constant assembly (polymerization) and disassembly (depolymerization) of microtubules, formed by a heterodimer constituted by α- and β-tubulin subunits,[3] plays a crucial role in mitosis and cell division where they are involved during the spindle formation, migration, cell shape organization, chromosomal separation and transportation of vesicles and mitochondria.[4] With a rather simple structure, CA-4 has shown to inhibit the polymerization of tubulin by binding to the colchicine site and thus, disrupting the tubulin-microtubule dynamics leading to mitotic arrest and eventually the cell death by apoptosis.[5] Nevertheless, the major drawbacks of CA-4 are its poor aqueous solubility, low bioavailability, cumulative toxicities and short biological half-life that have promoted its derivatization during the last decades.[6]

Several structure-activity relationship studies of CA-4 has revealed that the *cis* configuration of the double bond, the 3,4,5-trimethoxy groups on the A-ring, and the *meta*-hydroxy and *para*-methoxy groups on the B-ring are fundamental for its main biological activity.[7] Thereby,

CA-4 has inspired the synthesis and biological evaluation of different cytotoxic analogues containing these privileged pharmacophores: the disodium phosphate prodrug CA-4P **2**,[8] colchicine **3**,[9] podophyllotoxin **4**,[10] eugenol **5**[11] and some oxindole derivatives **6-7**[12] (Figure 1).

Besides the cytotoxic activity against a range of human cancer cell lines, in which CA-4 **1** induces the destabilization of proteins associated with the cytoskeleton, this compound is responsible for altering the coordination of many cellular processes, including the cell cycle, movement, adhesion, morphogenesis and contraction.[13] Several reports have determined that these cellular processes are involved in different infection processes of some pathogens such as bacteria,[14] parasites,[15] fungi[16] and viruses.[17]

In particular, CA-4 and some analogues have exhibited antifungal and antiviral activities whose mechanism of action involves the inhibition of tubulin polymerization or arrest of the cell cycle at different stages. For example, synthetic combretastatin analogues have exhibited relevant activity against *Trichophyton rubrum*, *Trichophyton mentagrophytes*, *Aspergillus fumigatus* and *Saccharomyces cerevisiae* through the regulation of signaling pathways.[18]

On the other hand, the use of microtubule inhibitors before the viral infection and during various phases of the virus life cycle, delays the intracellular transport of virions leading to the accumulation of viral particles at intracellular level.[19,20] In fact, ribonucleic acid (RNA) and deoxyribonucleic acid (DNA) viruses regulate microtubule during the different stages of the replicative cycle. For example, microtubule-associated proteins such as dynein, kinesin as well as dynactin 1 direct the transport of human herpesviruses serotype 1 (HHV-1), a DNA virus, inside the cell (dynactin subunit 1 (DCTN1)).[21] In the case of RNA viruses, it has been described the role of microtubules in early stages of infection of human immunodeficiency virus (HIV). Additionally, the flaviviruses use these structures to promote a reconfiguration of the cytoplasmic compartments that are important for the genome replication and translation of viral protein.[22]

Considering both the previously described data[23] regarding viral modulation of microtubules and the current need to research on synthesis and biological evaluation of small molecules inspired on the structure of CA-4 **1**, our screening program for new bioactive heterocycles[23] has focused this research on: (*i*) design and synthesis of a 20-member library of styrene and spiroisatin hybrids containing the 3,4,5-trimethoxyphenyl and/or the 4-hydroxy-3-methoxyphenyl as pharmacophoric subunits; (*ii*) evaluation of the cytotoxic activity in tumor cell lines (HeLa (cervix epitheloid adenocarcinoma cell), Jurkat (acute T cell leukemia), U937 (promonocytic cell) and Vero (African green monkey kidney, *Cercopithecus aethiops*)); (*iii*) study of the antifungal activities in pathogen dermatophytes (*T. mentagrophytes*, *T. rubrum* and *F. oxysporum*); (*iv*) determination of the antiviral activity in human herpesvirus 1 and 2 (HHV-1 and HHV-2), and dengue virus serotype 2 (DENV-2) of these molecules and some related tubulin inhibitors, and (*v*) the study of the possible interactions of these molecules with the active site of the tubulin target through molecular docking studies.

Results and Discussion

The preparation of the first library, the β-nitrostyrenes **10a**-**10c**, is shown in Scheme 1. The corresponding benzaldehydes **8a**-**8c** reacted with nitromethane **9** through a Knoevenagel condensation catalyzed by a ethanolamine supported on silica gel (ETAM/SiO$_2$) at 90 °C to furnish the styrene derivatives.[24]
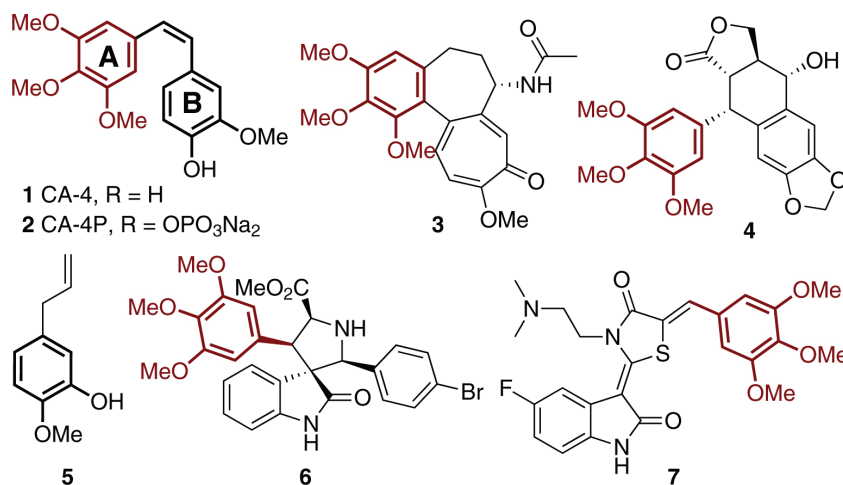
Figure 1. CA-4 (**1**) and some synthetic and natural derivatives (**2-7**) containing the pharmacophoric moieties related with its cytotoxic activity.
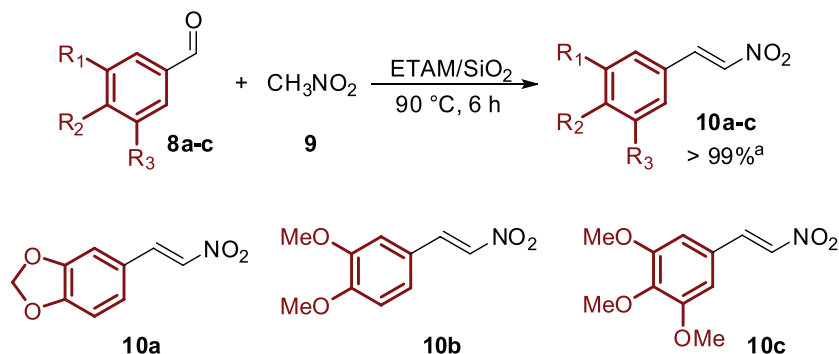
Scheme 1. Synthesis of β-nitrostyrenes **10a**-**10c** through a Knoevenagel condensation catalyzed by ethanolamine supported on silica gel (ETAM/SiO$_2$). Reaction conditions: **8a**-**8c** (5 mmol), **9** (20 mmol), catalyst (100 mg). [a]Products were obtained in quantitative yield and were purified by recrystallization.

The next group of molecules, the spiroisatin-dihydroquinoline hybrids **14a**-**14c** containing the 4-hydroxy-3-methoxyphenyl moiety, were synthesized through a two-step protocol in which the respective anilines **12a**-**12c** were condensated with isatin **11** to give the corresponding ketimine-isatin products. These intermediates were reacted in a second step with *trans*-isoeugenol **13** via Povarov reaction catalyzed by BF$_3$·OEt$_2$, given the desired adducts **14a**-**14c** in moderate yields (Scheme 2).[25]
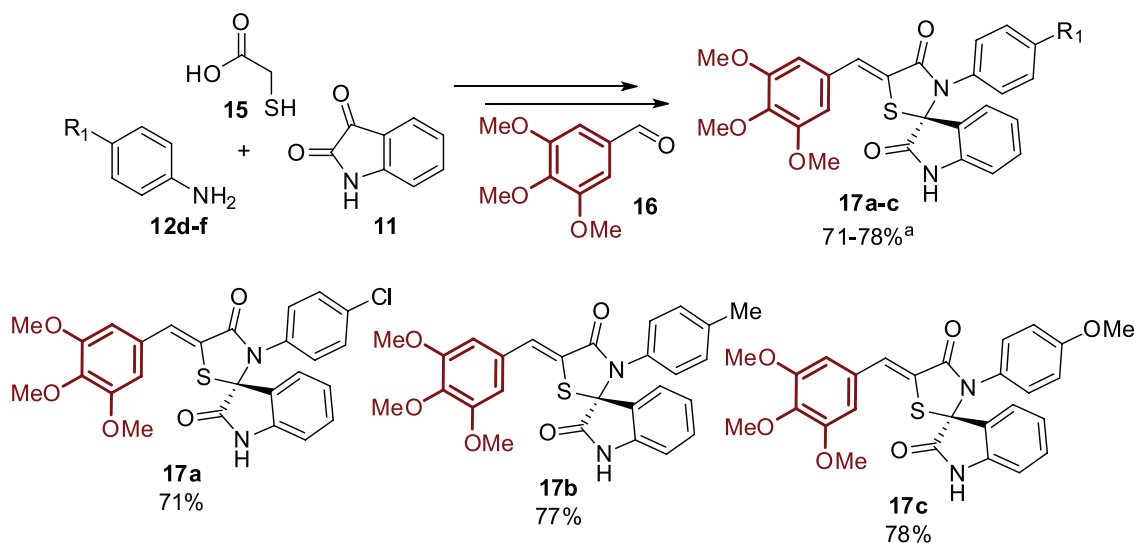
Next, the spiroisatin-thiazolidinone hybrids **17a**-**17c** containing the 3,4,5-trimethoxyphenyl moiety were prepared in another two-step synthetic methodology in which the first multicomponent reaction between isatin **11**,

anilines **12d**-**12f** and thioglycolic acid **15** afforded the respective 2,3-disubstituted-4-thiazolidinones as intermediates (Scheme 3). Then, the latter compounds underwent a Knoevenagel condensation catalyzed by *t*-BuOK at 90 °C with 3,4,5-trimethoxybenzaldehyde **16**, leading to the desired compounds **17a**-**17c** in good yields (Scheme 3).

Finally, the spiroisatin-nitropyrrolizidine hybrids **20a**-**20k** were synthesized through a multicomponent and regioselective 1,3-dipolar cycloaddition between isatin derivatives **18a**-**18c**, L-proline **19** and the β-nitrostyrenes **10a**-**10c** under aqueous media to furnish the title compounds **20a**-**20k** with the 3,4,5-trimethoxyphenyl moiety in excellent yields (Scheme 4).[26]
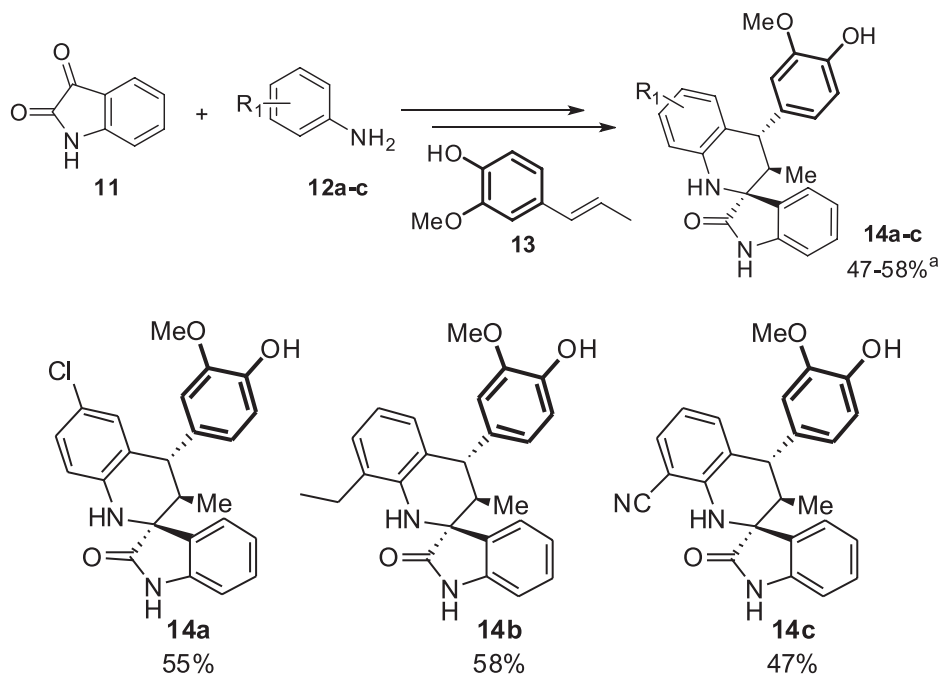
Scheme 2. Two-step synthesis of spiroisatin-dihydroquinoline hybrids **14a**-**14c** through a Povarov reaction with *trans*-isoeugenol **13**. Reaction conditions: first step: **11** (4 mmol), **12** (4.8 mmol), AcOH (5 equiv.) in MeOH (40 mL) at 70 °C for 8 h; the precipitated product (ketimine-isatin) was filtered and washed with petroleum ether; second step: ketimine-isatin (2 mmol), BF3·OEt$_2$ (2 mmol), *trans*-isoeugenol **13** (3 mmol) in CH$_2$Cl$_2$ (20 mL) at room temperature for 5 h under inert atmosphere. [a]Products were purified by recrystallization.

Scheme 3. Two-step synthesis of spiroisatin-thiazolidinone hybrids **17a**-**17c** through a Knoevenagel type condensation with 3,4,5-trimethoxybenzaldehyde **16**. Reaction conditions: first step: **11** (4 mmol), **12d**-**f** (4.2 mmol), **15** (6 mmol), AcOH (3 equiv.) in toluene (40 mL) at 110 °C for 8 h; the precipitated product (spirothiazolidinone) was filtered and washed with petroleum ether; second step: spirothiazolidinone (2 mmol), 3,4,5-trimethoxybenzaldehyde **16** (2.5 mmol) and *t*-BuOK (3 mmol) in isopropanol (IPA) (15 mL) at 90 °C for 5 h under inert atmosphere. [a]Products were purified by recrystallization.

In total, 20 molecules, having the main pharmacophoric moieties of CA-4 **1**, were prepared following our described synthetic procedures.[25,26] All of these small molecules were fully characterized, confirming their structure and stereochemistry by 1D (¹H and ¹³C)/2D (correlation spectroscopy (COSY), heteronuclear multiple bond correlation (HMBC), and heteronuclear single quantum correlation (HSQC)) nuclear magnetic resonance (NMR), infrared (IR) and mass spectroscopies; ensuring their purity before they were tested on the biological assays described below.

The target compounds **10a**-**10c**, **14a**-**14c**, **17a**-**17c** and **20a**-**20k** and the reference compounds CA-4 **1**, colchicine **3** and doxorubicine (adriamycin), were evaluated first for their *in vitro* anti-proliferative activities (cytotoxicity) against three different human tumor cell lines: cervix epitheloid adenocarcinoma cell (HeLa), acute T cell leukemia (Jurkat) and promonocytic cell (U937), as well as, the non-tumor cell line Vero (African green monkey kidney, *Cercopithecus aethiops*). For the determination of half maximal inhibitory concentration (IC₅₀) values, we used the *in vitro* tetrazolium dye assay (3-(4,5-dimethylthiazol-2-yl)-2,5-diphenyl tetrazolium bromide, MTT) according to our modified protocol.[27]

As shown in Table 1, compounds **17a**-**17c** and **20a**-**20k** did not exhibit significant anti-proliferative activities against different cancer cell lines, with an IC₅₀ value superior to 25 μM.[28] However, the substituted β-nitrostyrenes **10a**-**10c** showed activity against HeLa and Jurkat tumor cells, being compounds **10b** and **10c** the most active derivatives among the tested compounds on the HeLa tumor line with

IC₅₀ values of 16.4 and 10 μM, respectively. Nonetheless, the selectivity index (SI) was not significant with respect to the controls (**1**, **3** and doxorubicine (DOX)) (Table 1). Moreover, the β-nitrostyrene **10a** resulted to be active only for the Jurkat tumor cell line with an IC₅₀ value of 14 μM and with an SI of 2.4, being the higher magnitude among the series **10a**-**10c**, which were active and demonstrated a dose-dependent inhibition of the growth of cell lines. In addition, the spiroisatin-dihydroquinoline hybrids **14a** and **14c** were selective and active against one tumor cell line. Compound **14c**, which contains a cyanide moiety in the tetrahydroquinoline core and the 4-hydroxy-3-methoxyphenyl pharmacophoric unit, exhibited a high cytotoxic activity on U937 cell line with an IC₅₀ value of 13.5 μM.

Furthermore, the SI value of **14c** (SI = 6) resulted to be higher than the ones shown by the positive controls CA-4 **1** (SI = 4.9 for HeLa), colchicine **3** (SI = 0.1 for HeLa, SI = 2.1 for Jurkat and SI = 0.3 for U937) and doxorubicine (SI = 2.4 for HeLa); suggesting that compound **14c** could be considered as a possible antitumor agent (Table 1).

The *in vitro* antifungal activity was evaluated following the Clinical and Laboratory Standards Institute M38-A,[29] protocol for filamentous fungi, with some modifications.[30] The target compounds **10a**-**10c**, **14a**-**14c**, **17a**-**17c** and **20a**-**20k**, with the reference controls amphotericin B and terbinafine, were evaluated against different dermatophytes: *Trichophyton mentagrophytes*, *Trichophyton rubrum* and the environmental fungi *Fusarium oxysporum* (Table 2).
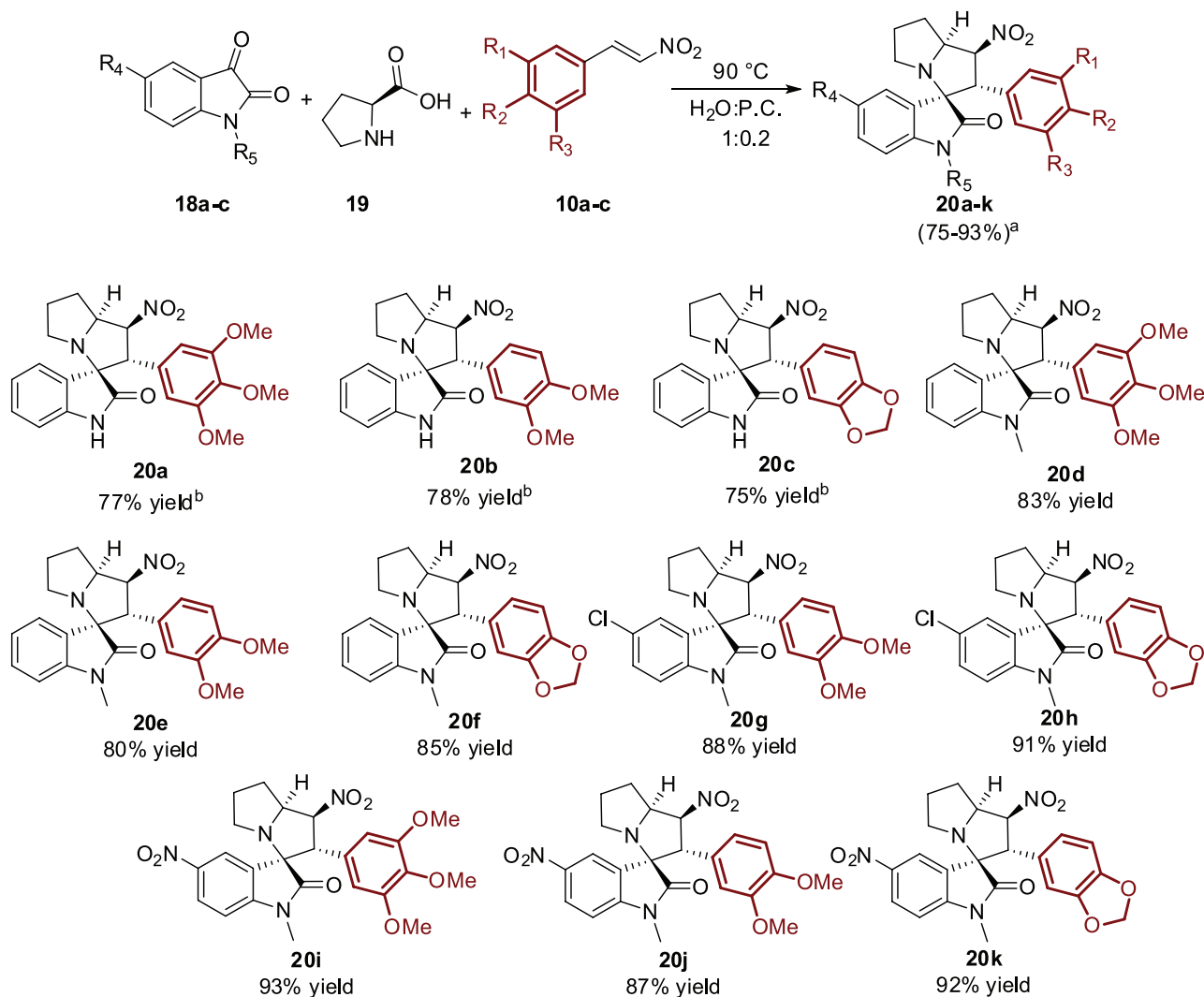
Scheme 4. Synthesis of spiroisatin-nitropyrrolizidine hybrids **20a-20k** through a regioselective 1,3-dipolar cycloaddition under aqueous media. Reaction conditions: **18a-c** (1 mmol), **19** (1.3 mmol), **10a-c** (1.1 mmol) in H_2O/PC (1:0.2) at 90 °C for 1 h. [a]Products were purified by SiO_2 column chromatography; [b]combined yield of the isolated mixture of regioisomers.

We found that among the all tested compounds in all the strains evaluated, only the group of β-nitrostyrenes **10a-10c** resulted to be active (minimal inhibitory concentration (MIC) ≤ 100 μM). These molecules were classified according to their MIC values as follows: **10c > 10b > 10a** (Table 2).

β-Nitrostyrene **10c** showed the most important antifungal activity against *T. mentagrophytes*, *T. rubrum* and *F. oxysporum* at concentrations 25.7, 40.6 and 32.4 μM, respectively. The activity of β-nitrostyrenes **10a-10c** against *F. oxysporum* outstands over the other strains because this fungus has been associated with systemic diseases that show high mortality rates and strong resistance to several antifungal agents.[31]

We have found in previous studies that some CA-4 **1** hybrids containing the (*Z*)-2-(3,4,5-trimethoxystyryl)

furan moiety have showed interesting antifungal activity against *T. mentagrophytes* and *T. rubrum*, giving MIC values of 15.7 ± 6.8 and 15.8 ± 6.5 μg mL^{-1}, respectively.[32] Furthermore, the antifungal activity of **10c** was previously determined against *C. albicans* ATCC 90028 giving an MIC value of 32.0 μg mL^{-1}.[33]

The results of this study confirm that the 3,4,5-trimethoxy phenyl moiety should be the fragment, which improves the antifungal activity, especially against *T. mentagrophytes*, allowing to conclude that this pharmacophoric subunit of CA-4 **1** is also relevant for the development of novel anti-dermatophytes agents.

Finally, the *in vitro* antiviral activity of all the synthesized compounds **10a-10c**, **14a-14c**, **17a-17c** and **20a-20k**, with the reference control acyclovir and CA-4, were evaluated against human herpesvirus 1 (HHV-1

Table 1. *In vitro* anti-proliferative activity (cytotoxicity) of all the synthesized compounds measured by the MTT test in four human tumor cell lines

Compound	Cell line[a]							
	HeLa		Jurkat		U937		Vero	
	$IC_{50} \pm SD^b$ / μM	SI^c	$IC_{50} \pm SD^b$ / μM	SI^c	$IC_{50} \pm SD^b$ / μM	SI^c	$IC_{50} \pm SD^b$ / μM	
1	19.91 ± 3.3	4.9	NT[f]	NT[f]	NT[f]	NT[f]	97.0 ± 0.7	
3	0.01 ± 0.001	0.1	0.0006 ± 0.00001	2.1	0.005 ± 0.001	0.3	0.001 ± 0.0001	
10a	> 25	NA[d]	14.0 ± 1.9	2.4	26.4 ± 0.2	1.3	33.1 ± 2.6	
10b	10.0 ± 1.06	1.6	12.5 ± 2.2	1.3	29.1 ± 0.7	0.5	15.7 ± 0.4	
10c	16.4 ± 0.46	0.8	> 25	NA[d]	28.2 ± 0.6	0.5	13.0 ± 0.4	
14a	> 25	NA[d]	> 25	NA[d]	14.7 ± 5.3	4.8	70.9 ± 1.1	
14b	> 25	NA[d]	> 25	NA[d]	> 25	NA[d]	> 25	
14c	> 25	NA[d]	> 25	NA[d]	13.5 ± 0.2	6.0	80.8 ± 2.98	
17a	> 25	NA[d]	> 25	NA[d]	> 25	NA[d]	> 25	
17b	> 25	NA[d]	> 25	NA[d]	> 25	NA[d]	> 25	
17c	> 25	NA[d]	> 25	NA[d]	> 25	NA[d]	> 25	
20a	> 25	NA[d]	> 25	NA[d]	> 25	NA[d]	> 25	
20b	> 25	NA[d]	> 25	NA[d]	> 25	NA[d]	> 25	
20c	> 25	NA[d]	> 25	NA[d]	> 25	NA[d]	> 25	
20d	> 25	NA[d]	> 25	NA[d]	> 25	NA[d]	> 25	
20e	> 25	NA[d]	> 25	NA[d]	> 25	NA[d]	> 25	
20f	> 25	NA[d]	> 25	NA[d]	> 25	NA[d]	> 25	
20g	> 25	NA[d]	> 25	NA[d]	> 25	NA[d]	> 25	
20h	> 25	NA[d]	> 25	NA[d]	> 25	NA[d]	> 25	
20i	> 25	NA[d]	> 25	NA[d]	> 25	NA[d]	> 25	
20j	> 25	NA[d]	> 25	NA[d]	> 25	NA[d]	> 25	
20k	> 25	NA[d]	> 25	NA[d]	> 25	NA[d]	> 25	
DOX[e]	0.8 ± 0.1	2.4	0.1 ± 0.007	19.0	0.1 ± 0.01	19.0	1.9 ± 0.08	

[a]HeLa: human cervix epithelial adenocarcinoma cells ATCC CRL-1958; Jurkat: human acute T cell leukemia ATCC TIB-152; U937: human promonocytic cell line ATCC CRL-1593.2; Vero: *Cercopithecus aethiops* African green monkey kidney cells ATCC CCL-81; [b]IC_{50}: concentration of the compound causing 50% cell growth inhibition after 48 h of compounds exposure, as determined by the MTT assay; [c]SI: selectivity index defined as VERO IC_{50} over either HeLa, Jurkat or U937 IC_{50}; [d]NA: not active; [e]positive control; [f]NT: not tested. SD: standard deviation.

CDC Atlanta acyclovir-sensitive strain) and human herpesvirus 2 (HHV-2 VR-734-G acyclovir-sensitive strain). The determination of the reduction factor (R_f), which corresponds to the value obtained by dividing the viral titer in the absence of compound over the viral titer obtained in the presence of compound was employed as an end point of this antiviral bioassay (Table 3).[34]

In a previous study carried out in our laboratory,[32] we reported the antiviral activity of combretastatin A-4 hybrid of HHV-2 at concentrations below 25.0 and 3.1 μg mL^{-1}. This background is important and establishes a guide for continue exploring antiviral activity.[32]

In order to determine the relevant or moderate antiviral activity of tested compounds, the reduction of R_f was established as a criterion to classify their potency according to the standard parameters.[30] Nevertheless,

only the spiroisatin-dihydroquinoline hybrids **14b**-**14c** exhibited moderate anti-herpetic activity, classifying them according to those parameters as follows: **14c** > **14b** > **14a**. Interestingly, the potency of compounds **14a**, **14b** and **14c**, with an R_f of 1×10^2, against HHV-2 at concentrations 25, 15.2 and 15.1 μM, respectively, can be correlated with the *in vitro* anti-proliferative activity of these compounds discussed above against U937.

It should be noted that the spiroisantin hybrids have a broad-spectrum biological activities, which involves antimicrobial.[35] In the particular case of the spiro[indoline-3,2'-quinolin]-2-one hybrid **14c**, it is clear that the presence of the nitrile (CN) moiety is important to improve the cytotoxic and the anti-herpetic activity, while the ethyl group and chlorine atoms at the same core decreases both activities.

Table 2. *In vitro* antifungal activity of all the synthesized compounds

Compound	Antifungal activity (MIC)[a,b] / μM		
	T. mentagrophytes	*T. rubrum*	*F. oxysporum*
10a	82.9	> 100	> 100
10b	59.8	59.8	59.8
10c	25.7	40.6	32.4
14a	> 100	> 100	> 100
14b	> 100	> 100	> 100
14c	> 100	> 100	> 100
17a	> 100	> 100	> 100
17b	> 100	> 100	> 100
17c	> 100	> 100	> 100
20a	> 100	> 100	> 100
20b	> 100	> 100	> 100
20c	> 100	> 100	> 100
20d	> 100	> 100	> 100
20e	> 100	> 100	> 100
20f	> 100	> 100	> 100
20g	> 100	> 100	> 100
20h	> 100	> 100	> 100
20i	> 100	> 100	> 100
20j	> 100	> 100	> 100
20k	> 100	> 100	> 100
Terbinafine	0.0268	0.0268	NT[c]

[a]Geometric means of minimal inhibitory concentration (MIC) of tested compounds; [b]the other positive control, amphotericin B, showed an antifungal activity of 1.1 μM against *A. fumigatus* and *A. flavus*; [c]NT: not tested.

Table 3. *In vitro* antiviral activity of all the synthesized compounds

| Compound	Vero cell line[a]			
	HHV-1		HHV-2	
	R_f[b]	Antiviral activity / μM	R_f[b]	Antiviral activity / μM
10a	NA[c]	NA[c]	NA[c]	NA[c]
10b	NA[c]	NA[c]	NA[c]	NA[c]
10c	NA[c]	NA[c]	NA[c]	NA[c]
14a	NA[c]	NA[c]	10^2	25
14b	NA[c]	NA[c]	10^2	15.1
14c	10^2	60.8	10^2	15.2
17a	NA[c]	NA[c]	NA[c]	NA[c]
17b	NA[c]	NA[c]	NA[c]	NA[c]
17c	10^2	99.1	NA[c]	NA[c]
20a	NA[c]	NA[c]	NA[c]	NA[c]
20b	NA[c]	NA[c]	NA[c]	NA[c]
20c	NA[c]	NA[c]	10^2	31.8
20d	NA[c]	NA[c]	NA[c]	NA[c]
20e	NA[c]	NA[c]	NA[c]	NA[c]
20f	NA[c]	NA[c]	NA[c]	NA[c]
20g	NA[c]	NA[c]	NA[c]	NA[c]
20h	NA[c]	NA[c]	NA[c]	NA[c]
20i	NA[c]	NA[c]	NA[c]	NA[c]
20j	NA[c]	NA[c]	NA[c]	NA[c]
20k	NA[c]	NA[c]	NA[c]	NA[c]
1	$10^{0.5}$	149.5	10^2	74.8
Acyclovir	10^4	6.7	10^4	6.7

[a]Vero *Cercopithecus aethiops* African green monkey kidney cell line ATCC CCL-81; [b]reduction factor: ratio of the virus titer in the absence over virus titer in the presence of the tested compound; [c]NA: not active. HHV-1: human herpesvirus 1 CDC Atlanta strain; HHV-2: human herpesvirus 2 VR-734-G strain.

Other compound that exhibited good antiviral activity belongs to the family of spiroisatin-nitropyrrolizidine hybrids **20a**-**20k**. With the 3,4-methylenedioxy phenyl moiety, the derivative **20c** resulted active against HHV-2, reducing to one hundred times the challenged viral load but at concentration of 31.8 μM. While the group of β-nitrostyrenes **10a**-**10c** showed no activity against human herpesviruses, the spiroisatin-thiazolidinone hybrids, **17c**, revealed effectiveness against HHV-1 at concentration 99.1 μM.

For anti-dengue activity, we highlight the effectiveness of the molecules **14a**, **14b** and **17c**. In this case, **14a** and **14b** molecules revealed an activity efficiency at a concentration of 30.2 and 29.7 μM, respectively (Figure 2). In addition, the **17c** molecule showed activity at various concentrations (198.2, 99.1 and 49.5 μM). Finally, for the antiviral assay with dengue virus, we employed ribavirin as control for each experiment.

The treatment with the **14a**, **14b** and **17c** molecules in dengue virus infected cells also caused visible morphological alterations under the microscope (data not shown), which are usually related to cytoskeleton remodeling. Several studies[36,37] have shown roles for tubulin during DNA and RNA viral infections, cancers and other pathological processes.

This would explain the broad spectrum of biological activity of the combretastatin hybrids included in this study, regarding CA-4 inhibitory activity in microtubule polymerization.

A key criterion for designing and developing new drugs is considering broad activity against medically important pathogens.

These results are important because the design and development of new drugs must take their activity spectrum into consideration, and a strong preference must be given to drug candidates that are active against the largest number
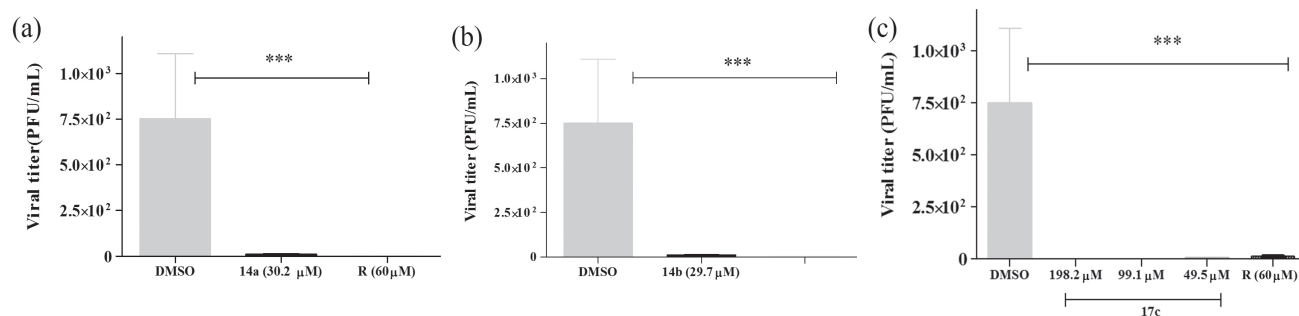
Figure 2. Molecules **14a**, **14b** and **17c** were effective in DENV-2 infection. BHK-21 cells were incubated in the presence or absence of **14a** (a); **14b** (b) and **17c** (c) molecules for six days and plaque forming units (PFU) were count, using as control ribavirin (R). Mean and SD: standard deviation compared to dimethyl sulfoxide (DMSO) and ribavirin control from three experiments are shown. *p*-Values were determined by two-tailed unpaired *t*-test (***: $p < 0.001$; **: $0.001 < p < 0.01$; *: $0.01 < p < 0.05$).

of co-circulating viruses and other pathogens that use the cell to perpetuate themselves and to cause pathology.

We carried out *in silico* assays using molecular docking to establish the mechanism of action of the tested molecules, that could explain their broad biological activities. The results showed molecules group **10a-c** binding to α-tubulin through hidrofobic interactions in the residues: Ala12, Tyr 224, Gln 11, Gly 144, Gly 10, Thr 145, Gly 146, Glu 183, Gly 142, Gly 143 and Ser 140 (Figures 3a-3c). The binding affinities (in kcal mol^{-1}) obtained were: **10a** (−7.2), **10b** (−6.7) and **10c** (−7.1) (Figures 3a-3c).

In addition, the molecules **14a-14b** were docked, and unlike the **10a-10c** compounds, these structures formed hydrogen bonds (Hb) with the α-tubulin. In the case of **14a**, the following Hb on the amino acids were shown: Leu 242,

Arg48 and Lys 96 (Figure 3d) and the **14b** showed Hb on Arg42 (Figure 3e). The Hb interactions have high stability which is relevant to explain the molecule activity. On the contrary, the compounds exhibited hydrophobic bindings that are less stable than Hb. Otherwise, the **14c** molecule interacts on the colchicine binding-site, nonetheless, the interactions are hydrophobic (Figure 3f).

The compound **17c** binds to subunit α/β-tubulin with an affinity −8.8 kcal mol^{-1} (Figure 3g). Interestingly, we observed an Hb on Arg 2 and Asn 50 residues. According with the crystallographic structure reported by Ravelli *et al.*[36] and Nogales *et al.*[38] the site of interaction between microtubules and compounds is different to the colchicine site. The results showed interaction in a region near to the nucleotide exchange area of tubulin, this is
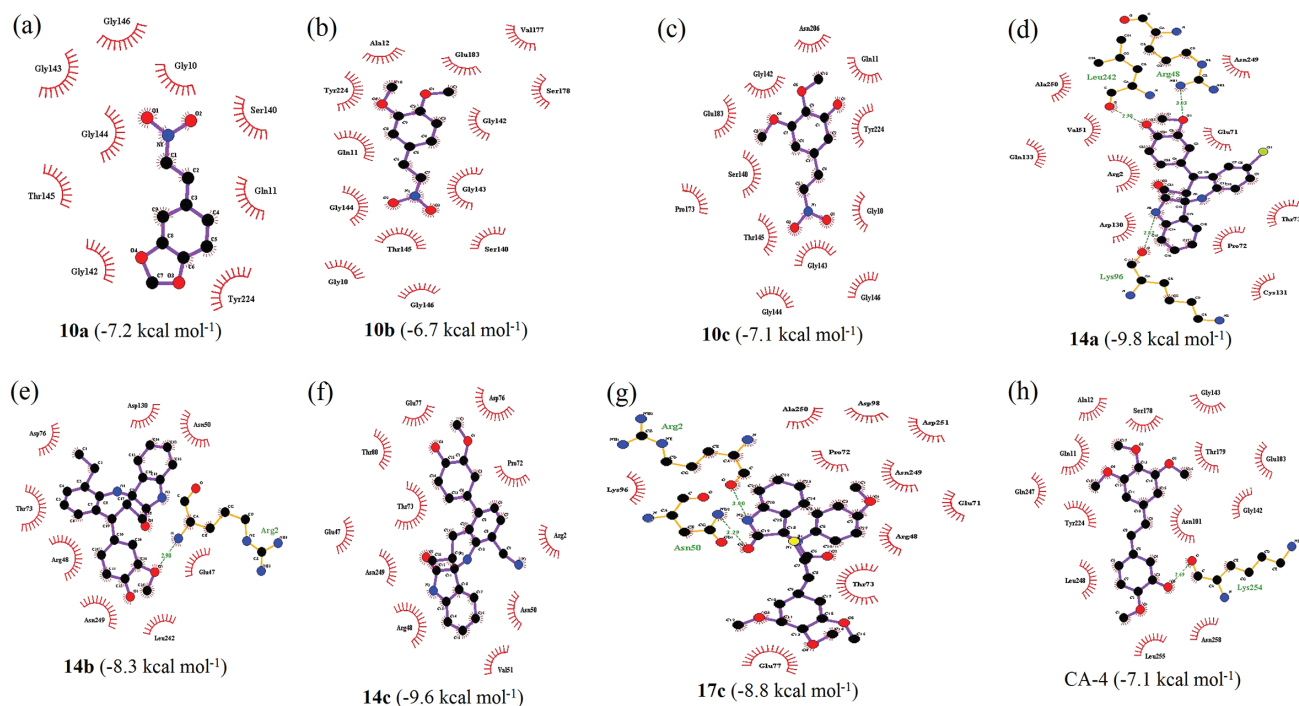
Figure 3. Molecular docking of molecules **10a-10c** (a-c); **14a-14c** (d-f); **17c** (g) and combretastatin A-4 (h). Each docking shows in parentheses the binding affinities expressed in kcal mol^{-1}. Hydrogen bounds are represented in a dotted line (green) and hydrophobic interactions are shown in red color.

relevant because the exchange of guanine nucleotide is required for the microtubule assembly.

Further, the control CA-4 was docked and as expected, it showed interaction in the colchicine binding site (Figure 3h). Finally, as perspective, we suggest biological validation of *in silico* results, i.e., to evaluate alterations in the tubulin pattern in a treatment context as well as determining if the possible changes are related to the biological activities reported here.

Conclusions

In this study, a series of styrene **10a**-**10c** and spiroisatin hybrids, containing the dihydroquinoline **14a**-**14c**, thiazolidinone **17a**-**17c** and nitropyrrolizidine **20a**-**20k** pharmacophoric subunits, were synthesized based on the structure of combretastatin A-4 **1**. The cytotoxicity, antifungal and antiviral activities of these libraries were evaluated for the first time.

Biological results revealed that among the diverse molecules tested with methoxy and/or hydroxy groups substituting the benzene rings, some compounds resulted active. β-Nitrostyrenes **10a**-**10c** exhibited notable data in two biological activities (cytotoxicity and antifungal); in particular, 3,4-dimethoxy-β-nitrostyrene **10b** displayed the highest cytotoxic activity among the tested series having the 3,4-methylenedioxy fragment.

Although none of the spiroisatin-thiazolidinone hybrids **17a**-**17c** exhibited representative activities (cytotoxic, antifungal or antiviral), our findings are relevant to encourage search of novel antitumoral, antifungal and antiherpetic agents. Additionally, the *in silico* studies demonstrated that these molecules could interact with tubulin in different areas compared to the colchicine binding site, suggesting a different mechanism of action.

Experimental

Chemistry

General procedure for the synthesis of β-nitrostyrenes **10a**-**10c**

Into a 10 mL round bottom flask equipped with a condenser, a gas bubbler and a stir bar, it was added the corresponding benzaldehyde **8a**-**8c** (5 mmol, 1 equiv.) and nitromethane **9** (20 mmol, 4 equiv.). The reaction mixture was stirred at 90 °C and 0.1 g of catalyst (ETAM/SiO$_2$) was added in one portion. The system was stirred at this temperature for six hours until the thin layer chromatography (TLC) monitoring confirmed the end of the reaction, then the reaction mixture was cooled at room

temperature and the catalyst was filtered and the filtrate was extracted three times with CH$_2$Cl$_2$ (3 × 20 mL). The organic layer was separated, dried with Na$_2$SO$_4$, and concentrated under reduced pressure to yield the pure product **10a**-**10c**. Characterization data for **10a**-**10c** is included in the Supplementary Information section associated to this article.

General method for the synthesis of spiroisatin-thiazolidinone hybrids **17a**-**17c**

A mixture of isatin **11** (4 mmol), the corresponding aniline **12d**-**12f** (4.2 mmol) and acetic acid (3 equiv.) in anhydrous toluene (40 mL) was refluxed for 3 h and thioglycolic acid **15** (6.04 mmol) was then added after 15 min. The reaction mixture was refluxed with a Dean-Stark apparatus for 8 h. After cooling, the reaction mixture was concentrated and added to a saturated NaHCO$_3$ solution. The obtained product, the spirothiazolidinone, was filtered and recrystallized. Without further purification, the respective intermediate (2 mmol), 3,4,5-trimethoxybenzaldehyde **16** (2.5 mmol) and potassium *tert*-butoxide (3 mmol) in isopropanol (IPA, 15 mL) was heated at 90 °C for 5 h under nitrogen atmosphere. TLC monitoring confirmed the end of the reaction, then the reaction mixture was cooled at room temperature and acetic acid (1 mL) was added. The precipitate was filtered and recrystallized to yield the desired products. Characterization data for **17a**-**17c** is included in the Supplementary Information section associated to this article.

General procedure for the synthesis of the spirooxindoles 1'-nitro pyrrolizidines **20a**-**20k**

Into a 15 mL round bottom flask equipped with a condenser, a gas bubbler and a stir bar, it was added the corresponding isatin **18a**-**18c** (2.50 mmol, 1 equiv.), the respective β-nitrostyrene **10a**-**10c** (1.1 equiv.), 1 mL of distilled water and 0.2 mL of propylene carbonate. The reaction mixture was stirred at 90 °C for 15 min prior to addition of the appropriate L-proline **19** (1.3 equiv.) and then the mixture was stirred at this temperature for one hour controlling the bubbling of CO$_2$. TLC monitoring confirmed the end of the reaction, then the reaction mixture was cooled at room temperature and quenched with saturated sodium bicarbonate solution (10 mL, 1 M) and was extracted three times with CH$_2$Cl$_2$ (3 × 20 mL). The organic layer was separated, dried with Na$_2$SO$_4$, and concentrated to afford the crude product, which was purified by silica gel flash chromatography to yield the corresponding spirooxindole 1'-nitro pyrrolizidines **20a**-**20k**. Characterization data for **20a**-**20k** is included in the Supplementary Information section associated to this article.

Biology

In vitro anti-proliferative activity assay

The *in vitro* anti-proliferative activities of CA-4 **1** and all of the target compounds were determined by the MTT (Sigma, New Jersey, USA) assay as described previously.[27] Briefly, Vero (african green monkey kidney, ATCC CCL-81) and HeLa (human cervix epithelial carcinoma, ATCC CRL-1958) cell lines were seeded into 96-well plates at 2.0×10^3 cells *per* well and incubated for 24 h at 37 °C. After the incubation time, each diluted compound was added to the appropriate wells and the plates were incubated for further 48 h at 37 °C in a humidified incubator with 5% CO_2. Jurkat (acute T cell leukemia human, ATCC TIB-152) and U937 (promonocytic, ATCC CRL-1593.2) cell lines were centrifuged to remove medium and were again suspended in culture medium and plated at 3×10^3 cells *per* well in a 96-well round-bottomed plate and diluted compounds were added to plates and incubated for 48 h at 37 °C. Subsequently, the culture medium was removed and the MTT solution (24 μL, 2 mg mL^{-1}) was added to each well. The minimal dilution of compound that induced 50% growth inhibition of the cells was expressed as inhibitory concentration 50% (IC_{50}). The IC_{50} values for each compound were obtained by linear regression analysis of the dose-response curves generated from the absorbance data with the statistical package R.[39] IC_{50} values were expressed as the mean ± standard deviation (mean ± SD) of two independent experiments done in quadruplicate. Also, the selectivity index (SI) was calculated.

In vitro antifungal activity assay

The dilutions of the compounds were dispensed into 96-well flat-bottom microdilution plates in duplicate at final concentrations between 100-20 μM. Amphotericine B was used as control with *Aspergillus fumigatus* and *Aspergillus flavus* at a range of 17.3-0.034 μM, and terbinafine with dermatophytes were used as positive controls at a range of 0.031-13.72 μM. The inoculum size for microdilution plates were $0.2-2.5 \times 10^5$ colony forming units (CFU) mL^{-1}. For the CLSI M38-A method,[29] the MICs were determined after 48 h of incubation at 35 °C to *Aspergillus* spp. and at 28 °C to *Fusarium oxysporum*. The activity against the dermatophytes was determined after 6 days of incubation at 28 °C.

In vitro antiviral activity assay

The anti-herpetic activity of molecules was evaluated on Vero cells against ten cell culture infectious dose fifty percent ($10TCID_{50}$) of HHV-1 and HHV-2, using the end-point titration technique (EPTT).[27] The activity was evaluated by determining the reduction factor (R_f) that corresponds to the ratio of viral titer treated with respect to titer viral untreated. For this assay, two independent experiments were carried out by quadruplicate and acyclovir was included as positive control. According to the established parameters,[27] the relevant or moderate antiviral activity of a purified natural product is one whose R_f of viral titer is $\geq 1 \times 10^3$ or 1×10^2, respectively.[28]

To determine the anti-DENV activity, baby hamster kidney (BHK-21) cell monolayers grown in 24-well plates 5.5×10^4 cells *per* well were infected with multiplicity of infection (MOI) = 1. Treatments were performed by adding compounds either simultaneously with virus (pre-infection treatment) or after viral infection (post-infection treatment). For pre-infection treatment, a virus/compound mixture was added to cell monolayers and was incubated for 2 h at 37 °C (5% CO_2). After incubation, a washing step was performed with phosphate buffered saline (PBS, pH 7.0) then it was added carboxymethyl cellulose (CMC) 1.5%. In post-infection treatment, virus was added on cell monolayer and incubated for 2 h at 37 °C (5% CO_2). After, washing was performed with PBS (pH 7.0), compounds previously prepared in CMC 1.5% were added and plates were incubated for six days. Cells were then fixed and stained with a solution of 3.5% formaldehyde with 0.2% crystal violet and viral plaques were counted. Dextran sulfate was employed as positive control in pre-infection assays. Ribavirin (RIBA) was used as positive control in post-infection stages of DENV-2. The fifty effective concentration (EC_{50}) was defined as the concentration that reduces the 50% of plaque forming units. EC_{50} for each compound were obtained by linear regression analysis of the dose-response curves generated using the statistical program GraphPad Prism 5.0.[40]

In silico (docking) studies

Molecular docking studies were perfomed using AutoDock Vina[41] to determine whether the synthesized compounds have comparable binding mode to that of CA-4 on the α,β-tubulin subunit that corresponds to the colchicine binding site. This area is formed by the following amino acids: α-tubulin: Thr179, Val 181, Ser 178; β-tubulin: Cys 241, Ala 250, Lys 254, Leu 255, Asn 258, Met 259, Ala 316, Ala 317, Lys 352, Thr 353, Ile 378.

In this study, the most active compounds (**10a-10c**, **14a-14c** and **17c**) were docked into colchicine binding site of the crystal structure of tubulin (PDB code: 3E22). For the visualization of interactions, it was employed LigPlot+ software.[42]

Supplementary Information

Acknowledgments

References

1. Chaudhary, A.; Pandeya, S. N.; Kumar, P.; Sharma, P. P.; Gupta, S.; Soni, N.; Verma, K. K.; Bhardwaj, G.; *Mini-Rev. Med. Chem.* **2007**, *7*, 1186.

2. Greene, L. M.; Meegan, M. J.; Zisterer, D. M.; *J. Pharmacol. Exp. Ther.* **2015**, *355*, 212.

3. Dumontet, C.; Jordan, M. A.; *Nat. Rev. Drug Discovery* **2010**, *9*, 790.

4. Etienne-Manneville, S.; *Curr. Opin. Cell Biol.* **2010**, *22*, 104.

5. Sanghai, N.; Jain, V.; Preet, R.; Kandekar, S.; Das, S.; Trivedi, N.; Mohapatra, P.; Priyadarshani, G.; Kashyap, M.; Das, D.; Satapathy, S. R.; Siddharth, S.; Guchhait, S. K.; Kundu, C. N.; Bharatam, P. V.; *Med. Chem. Commun.* **2014**, *5*, 766.

6. Ohsumi, K.; Nakagawa, R.; Fukuda, Y.; Hatanaka, T.; Morinaga, Y.; Nihei, Y.; Ohishi, K.; Suga, Y.; Akiyama, Y.; Tsuji, T.; *J. Med. Chem.* **1998**, *41*, 3022; Chen, J.; Liu, T.; Dong, X.; Hu, Y.; *Mini-Rev. Med. Chem.* **2009**, *9*, 1174.

7. Jin, Y.; Qi, P.; Wang, Z.; Shen, Q.; Wang, J.; Zhang, W.; Song, H.; *Molecules* **2011**, *16*, 6684.

8. Lippert III, J. W.; *Bioorg. Med. Chem.* **2007**, *15*, 605.

9. Lu, Y.; Chen, J.; Xiao, M.; Li, W.; Miller, D. D.; *Pharm. Res.* **2012**, *29*, 2943.

10. Sackett, D. L.; *Pharmacol. Ther.* **1993**, *59*, 163.

11. Jaganathan, S. K.; Mazumdar, A.; Mondhe, D.; Mandal, M.; *Cell Biol. Int.* **2011**, *35*, 607.

12. Antonchick, A. P.; Gerding-Reimers, C.; Catarinella, M.; Schürmann, M.; Preut, H.; Ziegler, S.; Rauh, D.; Waldmann, H.; *Nat. Chem.* **2010**, *2*, 735; Wang, S.; Zhao, Y.; Zhang, G.; Lv, Y.; Zhang, N.; Gong, P.; *Eur. J. Med. Chem.* **2011**, *46*, 3509.

13. Kanthou, C.; Tozer, G. M.; *Blood* **2002**, *99*, 2060; Hsu, L. C.; Durrant, D. E.; Huang, C. C.; Chi, N. W.; Baruchello, R.; Rondanin, R.; Rullo, C.; Marchetti, P.; Grisolia, G.; Simoni, D.; Lee, R. M.; *Invest. New Drugs* **2012**, *30*, 1379.

14. Gahlmann, A.; Moerner, W. E.; *Nat. Rev. Microbiol.* **2014**, *12*, 9.

15. Ferreira, D.; Cortez, M.; Atayde, V. D.; Yoshida, N.; *Infect. Immun.* **2006**, *74*, 5522; Jewett, T. J.; Sibley, L. D.; *Mol. Cell* **2003**, *11*, 885.

16. Takeshita, N.; Manck, R.; Grün, N.; de Vega, S. H.; Fischer, R.; *Curr. Opin. Microbiol.* **2014**, *20*, 34; Berepiki, A.; Lichius, A.; Read, N. D.; *Nat. Rev. Microbiol.* **2011**, *9*, 876.

17. Delorme-Axford, E.; Coyne, C. B.; *Viruses* **2011**, *3*, 2462; Sun, X.; Whittaker, G. R.; *Cell. Microbiol.* **2007**, *9*, 1672.

18. Coccetti, P.; Montano, G.; Lombardo, A.; Tripodi, F.; Orsini, F.; Pagliarin, R.; *Bioorg. Med. Chem. Lett.* **2010**, *20*, 2780.

19. Taylor, M. P.; Koyuncu, O. O.; Enquist, L. W.; *Nat. Rev. Microbiol.* **2011**, *9*, 427.

20. Mainou, B. A.; Zamora, P. F.; Ashbrook, A. W.; Dorset, D. C.; Kim, K. S.; Dermodya, T. S.; *mBio* **2013**, *4*, e00405; Dietzel, E.; Kolesnikova, L.; Maisner, A.; *Virol. J.* **2013**, *10*, 249.

21. Radtke, K.; Kieneke, D.; Wolfstein, A.; Michael, K.; Steffen, W.; Scholz, T.; Karger, A.; Sodeik, B.; *PLoS Pathog.* **2010**, DOI 10.1371/journal.ppat.1000991.

22. Naghavi, M. H.; Walsh, D.; *J. Virol.* **2017**, DOI 10.1128/JVI.00538-17.

23. Castro, M. A.; Gamito, A. M.; Tangarife-Castaño, V.; Roa-Linares, V.; del Corral, J. M. M.; Mesa-Arango, A. C.; Betancur-Galvis, L.; Francesch, A. M.; San Feliciano, A. S.; *RSC Adv.* **2015**, *5*, 1244; Martínez Bonilla, C. A.; Puerto Galvis, C. E.; Vargas Méndez, L. Y.; Kouznetsov, V. V.; *RSC Adv.* **2016**, *6*, 37478.

24. Mora, M.; Jiménez-Sanchidrián, C.; Urbano, F. J.; Ruiz, J. R.; *Catal. Lett.* **2010**, *134*, 131.

25. Kouznetsov, V. V.; Bello Forero, J.; Amado Torres, D. F.; *Tetrahedron Lett.* **2008**, *49*, 5855.

26. Puerto Galvis, C. E.; Kouznetsov, V. V.; *Org. Biomol. Chem.* **2013**, *11*, 7372.

27. Kouznetsov, V. V.; Merchán Arenas, D. R.; Tangarife Castaño, V.; Correa Royero, J.; Betancur Galvis, L.; *Med. Chem. Res.* **2016**, *25*, 429.

28. Cos, P.; Vlietinck, A. J.; Berghe, D. V.; Maes, L.; *J. Ethnopharmacol.* **2006**, *106*, 290.

29. Clinical and Laboratory Standards Institute (CLSI); Document M38-A: *Reference Method for Broth Dilution Antifungal Susceptibility Testing of Filamentous Fungi; Approved Standard*; CLSI: Wayne, USA, 2002.

30. Vlietinck, A. J.; Van Hoof, L.; Totté, J.; Lasure, A.; Berghe, D. V.; Rwangabo, P. C.; Mvukiyumwami, J.; *J. Ethnopharmacol.* **1995**, *46*, 31.

31. Triest, D.; Piérard, D.; De Cremer, K.; Hendrickx, M.; *Commun. Integr. Biol.* **2016**, *9*, e1162934.

32. González, M. A.; Pérez-Guaita, D.; Agudelo-Goméz, L. S.; Tangarife-Castaño, V.; Zapata, B.; Betancur-Galvis, L.; *Nat. Prod. Commun.* **2012**, *7*, 1051.

33. Pettit, R. K.; Pettit, G. R.; Hamel, E.; Hogan, F.; Moser, B. R.; Wolf, S.; Pon, S.; Chapuis, J. C.; Schmidt, J. M.; *Bioorg. Med. Chem.* **2009**, *17*, 6606.

34. Food and Drug Administration Center for Drug Evaluation and Research; *Guidance for Industry, Antiviral Product Development - Conducting and Submitting Virology Studies to the Agency*; U. S. Department of Health and Human Services, Rockville, USA, 2006.

35. Mohammadi, A. A.; Askari, S.; Rohi, H.; Soorki, A. A.; *Synth. Commun.* **2014**, *44*, 457.

36. Ravelli, R. B.; Gigant, B.; Curmi, P. A.; Jourdain, I.; Lachkar, S.; Sobel, A.; Knossow, M.; *Nature* **2004**, *428*, 198.

37. Naghavi, M. H.; Walsh, D.; *J. Virol.* **2017**, *91*, e00538-17.

38. Nogales, E.; Whittaker, M.; Milligan, R. A.; Downing, K. H.; *Cell* **1999**, *96*, 79.

39. *Software R*, version 4.0; Development Core Team, Vienna, Austria, 2008.

40. *GraphPad Prism 5.0*; GraphPad Software Inc., San Diego, CA, USA, 2009.

41. Trott, O.; Olson, A. J.; *J. Comput. Chem.* **2009**, *31*, DOI: 10.1002/jcc.21334.

42. Laskowski, R. A.; Swindells, M. B.; *J. Chem. Inf. Model.* **2011**, *51*, 2778.